Catalytic Behavior of Noble Metal Nanoparticle-Metal Oxide Assemblies: An Effect of Interfacial Ligands

Simantini Nayak and Yatendra S. Chaudhary

1 Introduction

The surface plasmonic resonance and catalytic properties exhibited by noble metal nanoparticles have allured great attention for their application, particularly in the catalysis [1–3]. Gold nanoparticles (Au NPs) exhibit high catalytic activity in contrast to bulk gold and hence are being exploited to catalyze various reactions such as propylene oxidation, water gas shift reaction, olefin epoxidation, and CO oxidation, etc [4–8]. However, the noble metal NPs are not stable and tend to collapse over a short period of time (a few hours) due to their high surface energy [22, 23]. An alternative approach developed to improve stability while retaining their catalytic activity is based on the dispersion of NPs on support materials. For example, Au NPs have been dispersed in both reducible oxides (TiO_2, ZnO, Fe_2O_3, CeO_2, ZrO_2, etc.) [9–11] and inert oxides (MgO, Al_2O_3, SiO_2) [12, 13]. Such Au NPs supports are conventionally synthesized from single-atom gold precursors using aqueous chemistry: by co-precipitation or deposition–precipitation methods [24]. Nonetheless, these approaches do not offer precise control over the size, size distribution, and degree of dispersion of Au NPs on the support.

The improved catalytic activity exhibited by such Au NPs-metal oxide support materials has been attributed to the size of Au NPs, NPs–metal oxide support interface and the surface defects of the support. Although the literature suggest that NPs-metal oxide support interface is the most active site for catalytic reactions, but, the role

S. Nayak · Y. S. Chaudhary (✉)
Materials Chemistry Department, CSIR-Institute of Minerals and Materials Technology, Bhubaneswar, Odisha 751013, India
e-mail: yschaudhary@immt.res.in

Y. S. Chaudhary
Academy of Scientific and Innovative Research (AcSIR), Ghaziabad 201 002, India

E. Chinthapudi et al. (eds.), *Sustainable Chemical, Mineral and Material Processing*, Lecture Notes in Mechanical Engineering,
https://doi.org/10.1007/978-981-19-7264-5_20

of interfacial interactions between NPs-metal oxide support has not been explored extensively.

To investigate the role of interfacial ligands/interactions between NPs-oxide support, the Au NPs were grafted on silica spheres using various kinds of interfacial functionalities such as amine, polyelectrolyte, and CTABr. These functionalities offer different nature of interfacial interactions ranging from electrostatic to coordination. SiO_2 is known to be a less active support for catalysis; however, we used SiO_2 in this study as support so that the catalytic activity is predominantly influenced by the interfacial interactions rather than the inherent activity of the support. Herein, the detailed results on the structural and CO oxidation activity of Au NPs-SiO_2 samples studied using TEM, FTIR, TPR, XPS, etc. are presented.

2 Material and Methods

2.1 Materials

Reagents used for the synthesis of silica spheres included TEOS (tetraethylorthosilicate) (98.0%, Aldrich), ethanol (99.9%, SDF Chem.), ammonia solution, and H2O (deionized, milli Q). For the synthesis of Au nanoparticles, Gold chloride trihydrate (ACS, Aldrich), Sodium citrate (Merck), Sodium borohydride (Merck), Cetyltrimethylammonium bromide (CTABr) (SDF Chem.), Ascorbic acid (Merck), and Sodium hydroxide (Merck) were used. All reagents were used as supplied.

2.2 Methods

2.2.1 Synthesis of Hydrolyzed Spherical Silica Spheres

Silica spheres were synthesized using Stober's process [14]. The obtained product was then calcined at 500 °C for 1 h. Since the calcinations lead to condensation of silanol groups, the calcined silica sphere samples were hydrolyzed to introduce hydroxyl groups for better functionalization. For this 1 g of the calcined powder was boiled with water in a 100 ml beaker with gentle stirring for 2 h. The obtained product was then centrifuged at 4000 rpm for 10 min and washed with deionized water for 3 times.

2.2.2 Synthesis of Au Nanoparticles

The citrate-stabilized and CTABr-capped Au NPs were synthesized by following the procedures reported in literature [15, 16]. Citrate stabilized Au precursor solution

was prepared by using $HAuCl_4$ and sodium citrate. CTABr-capped Au nanoparticle precursor solution was prepared by using the above Au precursor solution and a growth solution containing CTABr, $HAuCl_4$, and ascorbic acid and which was then kept for 12 h aging. After synthesis, CTABr-capped Au nanoparticles were centrifuged at 8000 rpm for 10 min and washed with deionized water for complete removal of the surfactant. The washing procedure was repeated for 4 times. The product obtained from 180 ml gold NP solution was resuspended in 5 ml of deionized water.

2.2.3 Anchoring of Au Nanoparticles onto Silica Spheres

To graft Au NPs, the hydrated silica spheres were functionalized with different functionalities. Using APTES (0.002 mol), silica sphere samples were functionalized with $–NH_2$ functionality. The other set of silica samples was functionalized with cationic polyelectrolyte (PE), using 1 ml of Poly(diallydimethylammonium chloride). 3 mg of $–NH_2$ and PE functionalized silica spheres were mixed with 6 ml of citrate-stabilized Au NP solution and allowed under equilibrium for 1 h which was followed by washing with deionized water and centrifugation. The Au NPs grafted silica sample having the functionalities of $–NH_2$ and PE are referred to as S-NH_2-Au and S-PE-Au, respectively, in the following text.

The grafting of CTABr-capped Au NPs onto silica spheres was carried out by the method reported by us by dispersing 50 mg of silica spheres in 5 ml of Au NP solution and sonicated for 1 min [17]. It was consequently stirred gently for 30 min at RT and allowed to stand for overnight at RT. The Au NP-silica spheres composites were recovered by centrifuging and washing with deionized water to ensure the absence of any unabsorbed Au NP solution. The completion of loading was confirmed by the absence of the absorption peak in the UV–Vis absorbance spectra taken for the supernatant solution. This sample is referred as S-CTABr-Au in the following text.

2.2.4 Characterization

The absorption spectra of Au nanoparticles and metal NP-functionalized silica spheres composites were recorded using a UV–Vis spectrophotometer (Shimadzu UV-2450). The morphology and size of silica spheres was examined by scanning electron microscope (Hitachi S-3400 N). The TEM analysis was done using a FEI Technai G2 20 microscope operated at 200 kV to determine the size and anchoring of Au NPs onto silica supports. The presence of different functional groups in the metal NP-silica sphere hybrids was confirmed using Fourier transform infra-red spectroscopy (Varian).

X-ray photoelectron spectroscopy (XPS) spectra were recorded by a VG Microtech ESCA 2000 Multilab spectrometer, equipped with a standard Mg Kα excitation source ($h\nu = 1253.6$ eV), and a hemispherical analyzer operating at constant pass energy of 20 eV. The binding energy (BE) scale calibration was done

by measuring C 1 s peak (BE = 284.6 eV) from the surface contamination and the accuracy was ± 0.9 eV. The differential surface charging of samples was ruled out by repeated scans under different X-ray exposures. All XPS data were fitted using the program of VGX-900, based on Gaussian peak shape after background subtraction.

The most reducing conditions of these Au-silica catalysts were examined by the analysis of temperature programmable reduction (TPR). Then the sample was subjected to heat treatment from RT to 700 °C under the 5% H_2/Ar (vol %) with a constant flow rate of 50 ml min^{-1}.

2.3 Catalytic Activity Evaluation

The catalytic activity of samples towards the oxidation of carbon monoxide was explored using a fixed bed flow reactor. 80 mg of samples were diluted with quartz and placed in the reactor. The reactant gas mixture consisting of CO (10%), O_2 (5%), and He (85%) at a flow rate of 40 ml min^{-1} was passed through the reactor. Analysis of effluent gases from the reactor was carried out using gas chromatography.

3 Results and Discussion

3.1 TEM Analysis

The silica sample synthesized using Stobers process lead to the formation of white powder which turned into light pink in color when grafted with Au NPs. To ensure the anchoring of Au NPs, the extent of surface coverage, and their structural details, TEM analysis was performed for all samples. The silica sample consists of monodisperse spheres of 320 ± 15 nm as can be seen in Fig. 1a, also SEM image is shown in supplementary information, Figure S1. The grafting of pre-fabricated Au NPs on silica spheres using different ligands is shown in Fig. 1b–d. The CTABr-capped Au nanoparticles are bigger in size, as expected, due to further growth of Au NPs while allowing them to age for longer time to ensure complete surface coverage by CTABr—as it was confirmed by FTIR spectrum (supporting information, Figure S2). The $–NH_2$ and PE functionalized silica spheres were found to have better coverage with Au NPs as compared to that achieved by CTABr-capped Au NPs onto silica spheres. In general, the grafted Au NPs were sturdily anchored onto silica spheres in case of all samples, as can be seen in the inset of Fig. 1b–d.

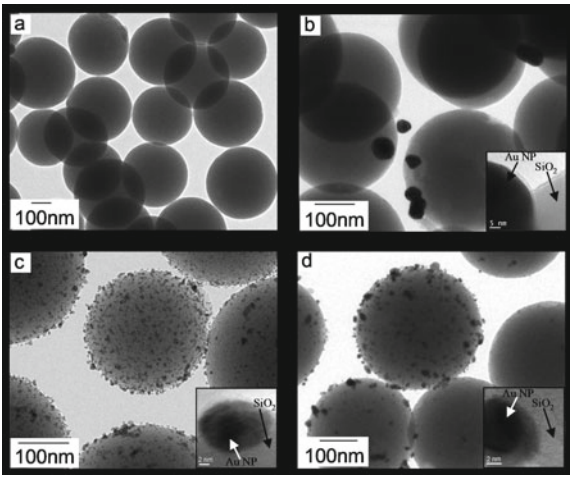

Fig. 1 TEM image of **a** silica spheres, **b** S-CTABr-Au, **c** S-NH_2-Au, **d** S-PE-Au, and inset shows their high magnification image of Au NP—support interface

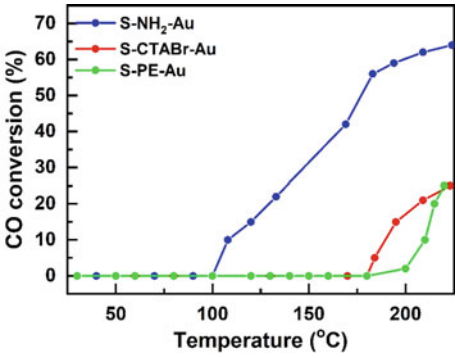

Fig. 2 CO oxidation as a function of temperature for Au NPs anchored silica sphere samples

3.2 CO Oxidation

To examine the catalytic activity and the effect of interfacial ligands of Au NPs grafted SiO_2 samples, CO oxidation was undertaken. The S-NH_2-Au shows CO oxidation at much lower temperature (starts at 100 °C) than that of reported in literature on non-reducing silica supports (ca ~ 270 °C) and lead to overall ~63% CO oxidation at 225 °C, Fig. 2. Whereas, in the case of both S-CTABr-Au and S-PE-Au, the CO oxidation starts at ca 180 °C and lead to ~25% CO oxidation at 225 °C, Fig. 2.

3.3 X-ray Photoelectron Spectroscopy (XPS)

In order to get an insight in such variation shown in the catalytic activity of these samples, XPS and TPR measurements were undertaken. XPS measurements were

performed for S-CTABr-Au, S-NH_2-Au, S-PE-Au catalysts to obtain further information about chemical state of Au species on the surface of the catalyst. All binding energy values given here have been charge corrected using the C1s line, Fig. 3. The binding energy (BE) values shown at 84.5 and 88.2 eV for S-CTABr-Au correspond to Au $4f_{7/2}$ and Au $4f_{5/2}$, thus suggesting the presence of Au^0 species [18, 19]. Whereas, two $4f_{7/2}$ components (at BE values of 86.6 and 90.1 eV) and two $4f_{5/2}$ components (at BE values 87.7 and 90.3 eV) observed for S-NH_2-Au indicate the presence of both, Au^{+1} and Au^{+3} species [18, 19]. The calculations done to determine the fractions of Au^{3+} and Au^{1+} present show that only 17.84% of the total gold present on S-NH_2-Au corresponds to Au^{+3} species. In the case of S-PE-Au, the BE values were observed at 85.7 and 89.3 eV which correspond to Au $4f_{7/2}$ and Au $4f_{5/2}$ and thus indicating the presence of Au^{1+} species.

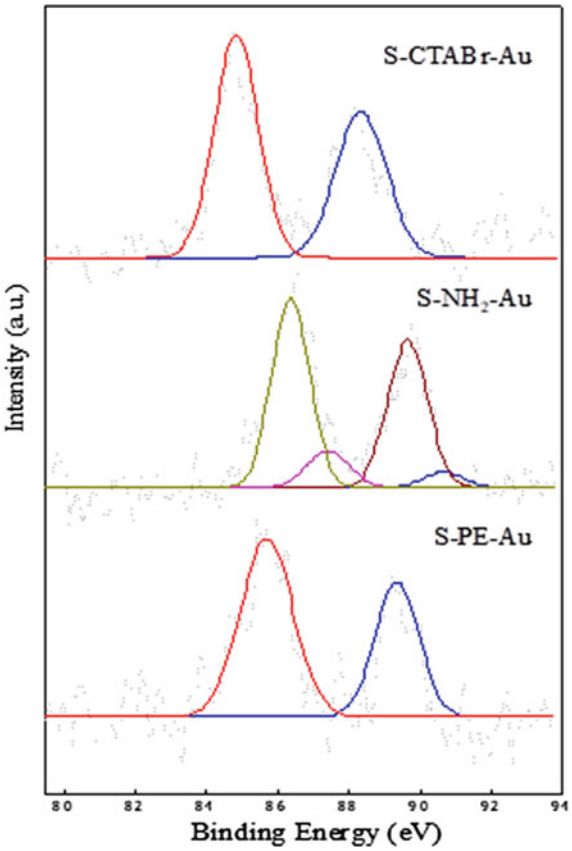

Fig. 3 XPS curve fitting of the Au 4f photoelectron peak in Au nanoparticle-silica samples

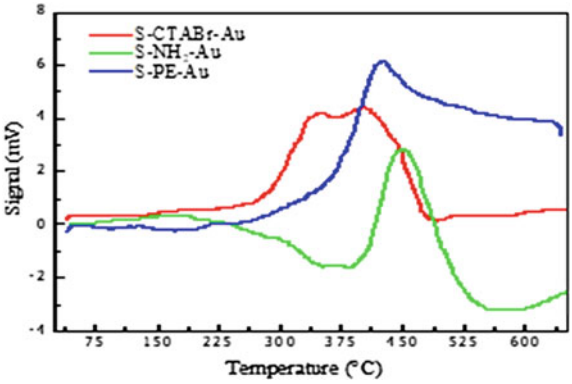

Fig. 4 Hydrogen TPR profile of Au NPs anchored silica sphere samples

3.4 Temperature Programmable Reduction (TPR)

The TPR profile of S-CTABr-Au demonstrates that the reduction of Au NPs initiated at lower temperature ca 259 °C than that of S-NH_2-Au (392 °C) samples, Fig. 4. The maximum reduction for these samples was observed at 346–403, 424, and 450 °C, respectively. The reduction taking place at higher temperature for S-NH_2-Au suggests strong binding of Au on silica spheres. Whereas, the S-CTABr-Au seems to have weekly bound Au NPs. The reduction taking place at moderate temperature 307 °C observed for S-PE-Au sample suggest weaker binding of Au NPs than that of S-NH_2-Au and stronger than that of S-CTABr-Au.

The CO oxidation observed at lower temperature for S- NH_2-Au is possibly due to better interaction of Au NPs with silica sphere supports which forms active interface. The presence of Au^{+1} species, as suggested by XPS data, plays an important role. It appears that it forms AuO- species at the interface which subsequently leads to significantly improved catalysis at lower temperature. The strong interfacial interaction between the Au NPs and the SiO_2 supports is also in compliance with the TPR data. The formation of such AuO- and consequently improved catalytic activity has also been observed with other oxide supports [20, 21]. The catalytic activity initiation at higher temperature that is 180 °C for S-CTABr-Au and S-PE-Au may be ascribed to weak interactions (as suggested by TPR data). S-CTABr exhibits very low catalytic activity at 180 °C which increases gradually till 200 °C and then increases exponentially. Such dual catalytic activity rate exhibited by S-CTABr-Au is complementary to the reduction behavior as shown by a broad peak having two maxima at 347 and 403 °C in TPR profile and may be attributed to the Au NPs shape effect. The synthesis of CTABr-Au NPs leads to elongated nanoparticles, as shown by the appearance of weak shoulder along with prominent peak in the absorption spectrum of CTABr-Au NPs (supporting information Figure S4). Therefore, Au NPs with such elongated shape may anchor in two different orientations and thus may exhibit different interface activity and consequently different catalytic activity.

4 Conclusion

In brief, the TPR study reveals that Au NPs exhibit the ascending interaction affinity order from S-CTABr-Au < S-PE-Au < S-NH_2-Au and interestingly the catalytic activity follows the same trend for all these samples. The CO oxidation observed at lower temperature for S-NH_2- is due to higher degree of the intimate interaction of Au NPs with silica sphere supports as compared to that of other S-PE-Au and S-CTABr. Furthermore, the dual catalytic activity rate observed in the case of S-CTABr-Au elongated nanoparticles enables the difference in the degree of the interaction between two different facets of nanoparticles. The CO oxidation, TPR, and XPS findings show that the interactions and the chemical state of the Au at the Au-support interface greatly influence the overall catalytic activity. These results on the interface tuning might have great implications on designing the catalysts for various commercially viable reactions.

Supporting Information

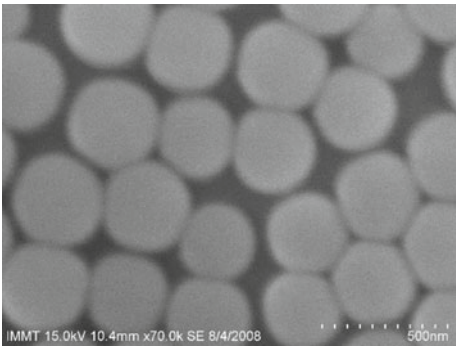

Figure S1 SEM image of silica spheres

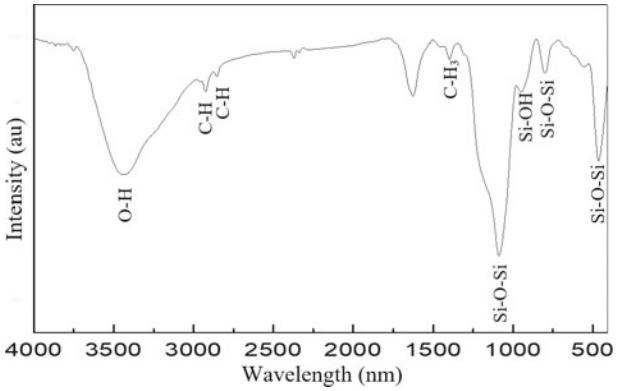

Figure S2 FTIR spectra S-CTABr-Au

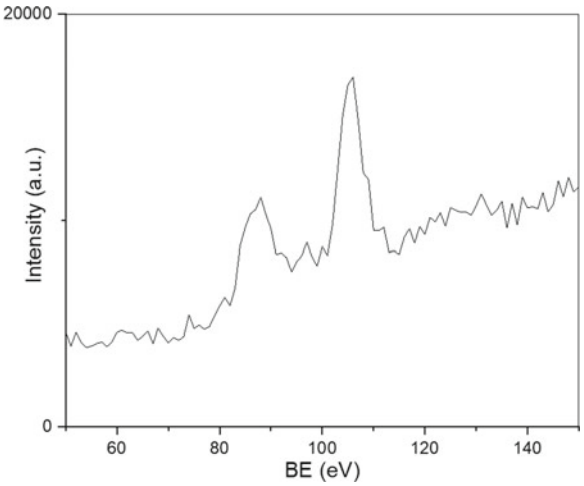

Figure S3 XPS Full survey spectrum of S-NH_2-Au

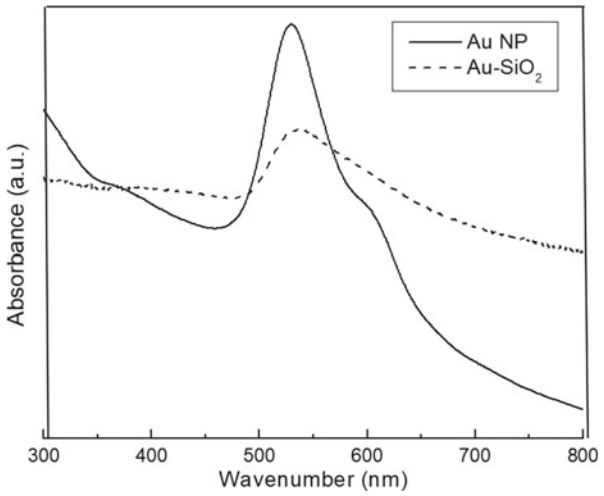

Figure S4 UV–Vis absorbance spectra of Au NP (capped with CTABr) before and after assembling steps

References

1. Warren SC, Thimsen E (2012) Plasmonic solar water splitting. Energy Environ Sci 5:5133
2. Haruta M, Daté M (2001) Advances in the catalysis of Au nanoparticles. Appl Catal A 222:427–437
3. Kim SH (2018) Nanoporous gold: preparation and applications to catalysis and sensors. Curr Appl Phys 18:810–818
4. Haruta M, Kobayashi T, Sano H, Yamada N, Novel (1987) Gold catalysts for the oxidation of carbon monoxide at a temperature far below 0 °C. Chem Lett 16:405–408
5. Haruta M, Yamada N, Kobayashi T, Iijima S (1989) Gold catalysts prepared by coprecipitation for low-temperature oxidation of hydrogen and of carbon monoxide. J Catal 115:301–309
6. Giorgi PD, Elizarov N, Antoniotti S (2017) Selective oxidation of activated alcohols by supported gold nanoparticles under an atmospheric pressure of O-2: batch and continuous-flow studies. ChemCatChem 9:1830–1836
7. Lomello-Tafin M, Chaou AA, Morfin F, Caps V, Rousset J (2005) Preferential oxidation of CO in H_2 over highly loaded Au/ZrO_2 catalysts obtained by direct oxidation of bulk alloy. Chem Commun 41:388–390
8. Reina TR, Ivanova S, Centeno MA, Odriozola JA (2016) The role of Au, Cu & CeO_2 and their interactions for an enhanced WGS performance. Appl Catal B 187:98–107
9. Ha H, Yoon S, An K, Kim HY (2018) Catalytic CO oxidation over Au nanoparticles supported on CeO_2 nanocrystals: effect of the Au–CeO_2 interface. ACS Catal 8:11491–11501
10. Kim HY, Lee HM, Henkelman G (2012) J Am Chem Soc 134:1560–1570
11. Han M, Wang X, Shen Y, Tang C, Li G, Smith RL Jr (2010) Preparation of highly active, low Au-loaded, Au/CeO_2 nanoparticle catalysts that promote CO oxidation at ambient temperatures. J Phys Chem C 114:793
12. Zhang Y, Zhang J, Zhang B, Si R, Han B, Hong F, Niu Y, Sun L, Li L, Qiao B, Sun K, Huang J, Haruta M (2020) Boosting the catalysis of gold by O_2 activation at Au-SiO_2 interface. Nat Commun 11:558

13. Hernández WY, Aliç F, Navarro-Jaen S, Centeno MA, Vermeir P, Voort PVD, Verberckmoes A (2017) Structural and catalytic properties of Au/MgO-type catalysts prepared in aqueous or methanol phase: application in the CO oxidation reaction. J Mater Sci 52:4727–4741
14. Stöber W, Fink A, Bohn E (1968) Controlled growth of monodisperse silica spheres in the micron size range. J Colloid Interf Sci 26:62–69
15. Petkov N, Stock N, Bein T (2005) Gold electroless reduction in nanosized channels of thiol-modified SBA-15 material. J Phys Chem B 109:10737–10743
16. Busbee BD, Obare SO, Murphy CJ (2003) An improved synthesis of high-aspect-ratio gold nanorods. Adv Mater 15:414–416
17. Chaudhary YS, Ghatak J, Bhatta UM, Khushalani D (2006) One-step method for the self-assembly of metal nanoparticles onto facetted hollow silica tubes. J Mater Chem 16:3619–3623
18. Casaletto MP, Longo A, Martorana A, Prestianni A, Venezia AM (2006) XPS study of supported gold catalysts: the role of Au^0 and $Au^{+\delta}$ species as active sites. Surf Interf Anal 38:215–218
19. Fu Q, Saltsburg H, Flytzani-Stephanopoulos M (2003) Active nonmetallic Au and Pt species on ceria-based water-gas shift catalysts. Science 301:935–938
20. Pestryakov AN, Lunin VV, Kharlanov AN, Kochubey DI, Bogdanchikova N, Stakheev AY (2002) Influence of modifying additives on electronic state of supported gold. J Mol Struct 642:129–136
21. Pestryakov AN, Lunin VV (2000) Physicochemical study of active sites of metal catalysts for alcohol partial oxidation. J Mol Catal A 158:325
22. Bachenheimer L, Elliot P, Stagon S et al (2014) Enhanced thermal stability of Ag nanorods through capping. Appl Phys Lett 105:213104
23. Sheng WC, Lee SW, Crumlin EJ, Chen S, Shao-Horn Y (2011) Synthesis, activity and durability of Pt nanoparticles supported on multi-walled carbon nanotubes for oxygen reduction. J Electrochem Soc 158:B1398–B1404
24. Priecel P, Salami HA, Padilla RH, Zhong ZY, Lopez-Sanchez JA (2016) Anisotropic gold nanoparticles: preparation and applications in catalysis. Chin J Catal 37:1619–1650